

1 **Strategies to Reduce Uncertainties from the Best Available**  
2 **Physicochemical Parameters Used for Modeling Novel**  
3 **Organophosphate Esters Across Multimedia Environments**

4 Changyue Xing<sup>1, 2</sup>, Jianxin Ge<sup>1, 2</sup>, Rongcan Chen<sup>1, 2</sup>, Shuaiqi Li<sup>1, 2</sup>, Chen Wang<sup>3</sup>,  
5 Xianming Zhang<sup>4</sup>, Yong Geng<sup>1</sup>, Kevin C. Jones<sup>5</sup>, and Ying Zhu<sup>1, 2\*</sup>

6 <sup>1</sup>School of Environmental Science and Engineering, Shanghai Jiao Tong University,  
7 Shanghai 200240, China

8 <sup>2</sup>The Key Laboratory of Environmental Health Impact Assessment for Emerging  
9 Pollutants, Ministry of Ecology and Environment of the People's Republic of China,  
10 Shanghai 200240, China

11 <sup>3</sup>Shenzhen Key Laboratory of Precision Measurement and Early Warning Technology  
12 for Urban Environmental Health Risks, School of Environmental Science and  
13 Engineering, Southern University of Science and Technology, Shenzhen, Guangdong  
14 518055, China

15 <sup>4</sup>Department of Chemistry and Biochemistry, Concordia University, 7141 Sherbrooke  
16 Street West, Montreal, QC H4B 1R6, Canada

17 <sup>5</sup>Lancaster Environment Centre, Lancaster University, Lancaster LA1 4YQ, United  
18 Kingdom

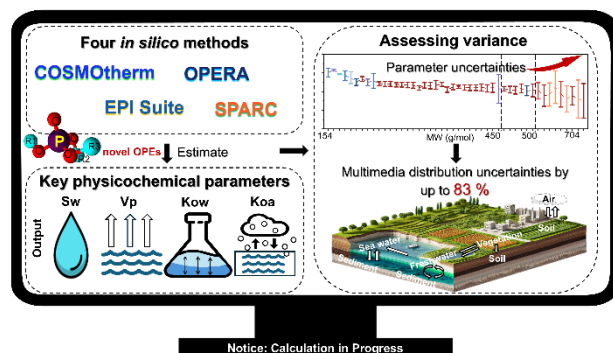
19  
20 \*Corresponding author

21 Email address: yzhu16@sjtu.edu.cn (Ying Zhu)

22

## 23 **Abstract**

24 Organophosphate esters (OPEs) raise growing environmental and human health  
25 concern globally. However, numerous novel OPEs lack data on physicochemical  
26 properties, which are essential for assessing environmental fate, exposure and risks.  
27 This study predicted water solubility ( $S_w$ ), vapor pressure ( $V_p$ ), octanol-water partition  
28 coefficient ( $K_{ow}$ ) and octanol-air partition coefficient ( $K_{oa}$ ) at 25 °C for 46 novel OPEs  
29 by identifying optimal *in silico* tools and establishing prediction strategies based on  
30 molecular weights (MWs). Prediction discrepancies between *in silico* tools increased  
31 with MWs and structural complexity. Method evaluations for compounds with  
32 MWs >450 g/mol suggest that COSMOtherm is advantageous in predicting  $S_w$  and  $V_p$   
33 for alkyl-OPEs, while SPARC is better for predicting  $V_p$  for aryl- and halogenated-  
34 OPEs. For compounds with MWs >500 g/mol, COSMOtherm and SPARC are  
35 recommended for  $K_{ow}$  and  $K_{oa}$  prediction, respectively. For smaller OPEs, average  
36 values from the top three of COSMOtherm, SPARC, EPI Suite and OPERA, ranked by  
37 validation on traditional flame retardants, are recommended. Using improper software  
38 could cause deviations in multimedia distribution and overall persistence in  
39 environment by up to 83% and 350%, respectively. The present data and prediction  
40 strategy are useful to enhance reliability of environmental fate, exposure and risk  
41 assessments of various OPEs and emerging contaminants.



42

43 **Synopsis:** Key physicochemical parameters are predicted for 46 novel  
 44 organophosphate esters lacking experimental data, and a prediction strategy is  
 45 established.

46 **Keywords:** novel organophosphate esters, physicochemical properties, water  
 47 solubility ( $S_w$ ), octanol-water partition coefficient ( $K_{ow}$ ), vapor pressure ( $V_p$ ), octanol-  
 48 air partition coefficient ( $K_{oa}$ ), environmental multimedia distribution, overall  
 49 persistence.

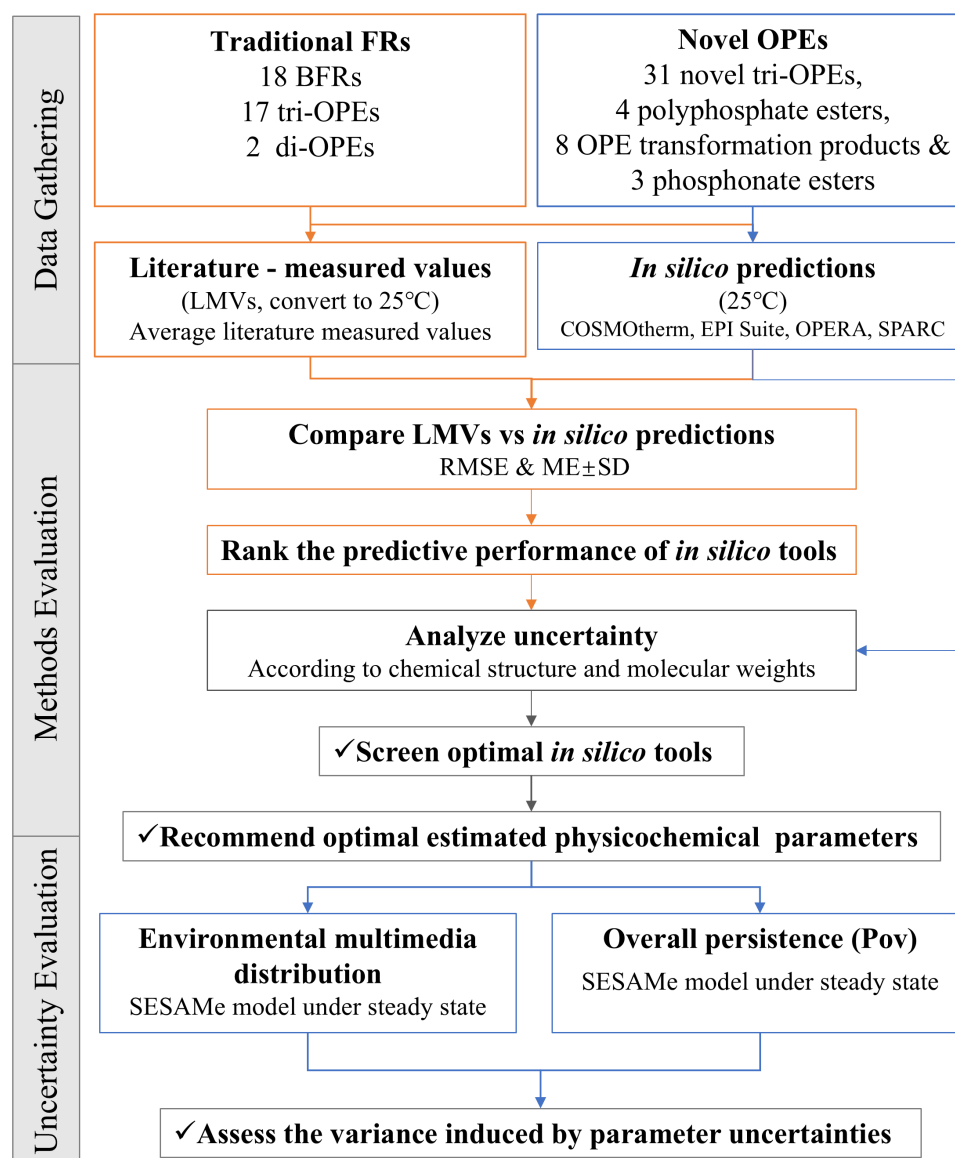
## 50 **Introduction**

51 Organophosphate esters (OPEs) are synthetic organic chemicals widely used as  
52 flame retardants (FRs) and plasticizers etc. in a wide variety of sectors such as  
53 construction, textiles, and electronics manufacturing.<sup>1,2</sup> Global production had grown  
54 to one million tonnes by 2018<sup>3</sup>, as they were initially marketed as “environmentally  
55 friendly” replacements of polybrominated diphenyl ethers (PBDEs) flame retardants.  
56 PBDEs have been listed under the Stockholm Convention in 2009 and 2017.<sup>3-6</sup> However,  
57 increasing evidence indicates that OPEs also have persistent, bioaccumulative and toxic  
58 (PBT) properties, raising concerns about their status as a “regrettable replacement”.<sup>7</sup>  
59 Furthermore, recent studies highlight additional risks from OPE environmental  
60 transformation products, which may exhibit higher toxicity than the parent compounds,  
61 as well as novel OPEs (NOPEs) derived from organophosphite antioxidants (OPAs).<sup>8-</sup>  
62 <sup>10</sup> Despite this, research on the physicochemical properties of these NOPEs remains  
63 scarce. OPEs are typical semi-volatile organic compounds (SVOCs) with diverse  
64 physicochemical properties.<sup>11</sup> Compound physicochemical properties, such as water  
65 solubility ( $S_w$ ), vapor pressure ( $V_p$ ) and octanol-water partition coefficient ( $K_{ow}$ ), are  
66 essential for understanding OPE multimedia distribution and their primary exposure  
67 routes to humans and environmental organisms.

68 *In silico* simulation tools have become essential for predicting physicochemical  
69 properties of substances for which experimental data and laboratory measurements are  
70 lacking. COSMOtherm,<sup>12</sup> EPI Suite,<sup>13, 14</sup> SPARC,<sup>14</sup> and OPERA<sup>15</sup> etc. are examples of  
71 software tools that have been extensively used for compounds including

72 polychlorinated biphenyls (PCBs), PBDEs, per- and polyfluoroalkyl substances (PFAS),  
73 and certain OPEs well-studied as FRs (often referred to as “traditional” chemicals).<sup>16-</sup>  
74 <sup>22</sup> Each tool exhibits varying performance across different chemicals and properties.  
75 For instance, COSMOtherm has demonstrated superior accuracy in predicting  $S_w$ ,  $V_p$   
76 for PBDEs and PFAS, and  $K_{ow}$ , octanol-air partition coefficient ( $K_{oa}$ ), air-water  
77 partition coefficient ( $K_{aw}$ ) for PCBs and PFAS.<sup>16-21</sup> Meanwhile, SPARC has performed  
78 well for  $K_{ow}$  and  $K_{aw}$  predictions for brominated flame retardants (BFRs), while  
79 OPERA has excelled at  $S_w$ ,  $K_{ow}$ , and  $K_{oa}$  predictions for traditional OPEs.<sup>21, 23</sup> EPI Suite  
80 could provide parameter estimates that allow for more accurate calculation of  $K_{aw}$  for  
81 traditional OPEs.<sup>17</sup> In a screening study conducted by Zhang et al. (2010) using four  
82 software applications, consistent predictions for bioaccumulation and long-range  
83 transport potential across the four tools were obtained for only 70% of 529 substances  
84 analyzed, highlighting significant variability among the software applications.<sup>24</sup>

85 This study aims to identify the optimal *in silico* tools for predicting  $V_p$ ,  $S_w$ ,  $K_{ow}$ ,  
86  $K_{oa}$  for 46 NOPEs. Uncertainties of chemical multimedia distribution and overall  
87 persistence induced by variability of physicochemical parameters are illustrated by a  
88 well-developed and validated multimedia environmental fate model developed for  
89 China. This work highlights the impact of selecting inappropriate software on chemical  
90 fate predictions, which has rarely been discussed and demonstrated quantitatively  
91 before. The study provides valuable data and insights for researchers conducting either  
92 experimental or modelling research on environmental fate, exposure, and health risks  
93 of OPEs and other chemicals.



95

96

**Figure 1.** Flowchart of the workflow.

97 Figure 1 demonstrates the workflow and method of this study, with details stated as  
 98 follows.

### 99 **Chemical selection and data gathering.**

100 Two groups of chemicals were included in this study: Group (1) consists of 37  
 101 traditional FRs for model evaluation, including 18 BFRs and 19 traditional OPEs (5  
 102 aryl-organophosphate triesters (tri-OPEs), 7 alkyl-tri-OPEs, 5 halogenated-tri-OPEs

103 and 2 alkyl-organophosphate diesters (di-OPEs)); and Group (2) comprises 46 NOPEs  
104 without reported experimental data of above physicochemical parameters, including 31  
105 novel tri-OPEs, 4 polyphosphate esters, 8 environmental transformation products of  
106 OPEs and 3 phosphonate esters. The targeted OPE transformation products, except  
107 MDPP and 2,4DtBP (phenol), are di-OPEs. The pairing of OPEs and their  
108 transformation products is shown in Figure S1 in the Supporting Information (SI).

109 Information of chemicals in Group (2) is given in SI Text S1 and Tables S1-S2.  
110 Most NOPEs are primarily used as flame retardants and plasticizers (Table S2). Some  
111 of them are commercially used as alternatives to traditional organophosphate FRs. For  
112 example, o-CDPP, m-CDPP, P-CDPP (the isomers of CDPP), RDP, IDDPP, BPDPP and  
113 BPA-BDPP are replacements of TPHP while V6 and RDP are the alternatives to TEP,  
114 TCEP and TCIPP.<sup>1, 25</sup> Additionally, four NOPEs, i.e. AO168=O, TNPP, TiDeP,  
115 AO626=O<sub>2</sub>, are oxidation products of OPAs. While AO168=O is used as a processing  
116 stabilizer for polymers in limited quantities, there is no direct industrial application for  
117 the other NOPEs (Table S2).<sup>25, 26</sup> Many of the target OPE transformation products also  
118 have direct production for industrial application (Table S2). The three phosphonate  
119 esters (DEEP, mono-PMMMP and di-PMMMP) have been newly identified in  
120 environmental matrices; and meanwhile, mono-PMMMP and di-PMMMP are  
121 transformation products of widely-used commercial organophosphate esters containing  
122 phosphorus-oxygen or phosphorus-sulfur bonds, probably exhibiting high  
123 environmental abundance.<sup>27, 28</sup> Some NOPEs have been detected in various  
124 environmental media and wildlife, with concentrations higher or comparable to those

125 of traditional OPEs.<sup>25, 29-32</sup> A few of them have demonstrated high acute or chronic  
126 toxicity to aquatic organisms, such as BPA-BDPP and CDPP.<sup>33, 34</sup>

127 The chemical selection in Group (1) has covered the functional groups contained  
128 in the compounds in Group (2) (Table S3) for better representativeness and reasonable  
129 guidance in identification of the optimal model for novel compounds. The molecular  
130 weights (MWs) range from 140 to 959 g/mol, reflecting a broad variation of chemical  
131 structural complexity. The literature-derived data of physicochemical parameters for  
132 the 37 traditional compounds in Group (1) were compiled and further harmonized to  
133 only include more reliable experimental data for better validation of the *in silico* tools,  
134 given that laboratory measurements may also have uncertainties.<sup>35</sup> The selection of  
135 literature-derived experimental data referred to the suggested rules by previous studies,  
136 such as the standardization of experimental methods and reasonable parameter ranges  
137 obtained by specific experimental methods etc (Table S4).<sup>35, 36</sup> Subsequently, to ensure  
138 thermodynamic consistency across the dataset, the literature values not originally  
139 measured at 25°C were converted to this temperature using equation S1, thereby  
140 unifying all values to reflect measurements at 25°C.<sup>21, 37</sup> If more than one value was  
141 found for individual parameters of each chemical, the average values were taken for the  
142 validation. The detailed method and selected experimental data are given in the SI Text  
143 S2 and Tables S5-S8.

#### 144 ***In silico* prediction of physicochemical properties and method evaluation.**

145 For all traditional and novel compounds,  $S_w$ ,  $V_p$ ,  $K_{ow}$ , and  $K_{oa}$  at 25 °C were  
146 predicted using COSMOtherm (BIOVIA COSMOtherm 2021, version 21.0), EPI Suite



147 (the U.S. EPA's Estimation Programs Interface Suite, version 4.11), OPERA (OPEn  
148 structure-activity/property relationship application, version 2.9), and SPARC (SPARC  
149 Performs Automated Reasoning in Chemistry).<sup>12-15</sup> The modules used in EPI Suite for  
150 each parameter are specified in the SI Text S3, and WATERNT was adopted to predict  
151 the  $S_w$  for its better reliability than WSKOW (Table S9). Only OPERA can directly  
152 predict  $K_{oa}$ , using a machine learning algorithm based on the weighted k-nearest  
153 neighbor (KNN) model.<sup>15</sup> The EPI Suite KOAWIN model can output  $K_{oa}$ ; however, this  
154 is not a direct calculation but follows the same principle as the other two software  
155 applications.  $K_{oa}$  is calculated based on  $K_{aw}$  and  $K_{ow}$  as shown in equations 1-2 (Eqs 1-  
156 2).  $H$  and  $R$  represent the Henry's law constant and the gas constant, respectively.  $T$  is  
157 the temperature.

$$158 \quad K_{aw} = \frac{H}{RT} \quad (1)$$

$$159 \quad K_{oa} = K_{ow} / K_{aw} \quad (2)$$

160 EPI Suite v4.11 and OPERA are based on the principle of quantitative structure-  
161 activity relationship (QSAR) models. QSAR models predict based on mathematical  
162 relationships between chemical structures and their physicochemical properties or  
163 biological activities. These models are trained on existing datasets to develop regression  
164 models that can predict properties of unmeasured compounds. OPERA utilizes a  
165 machine learning model based on weighted k-nearest neighbors (KNN) algorithm,  
166 incorporating molecular descriptors from the Pharmaceutical Data Exploration  
167 Laboratory (PaDEL). Descriptor selection is performed using genetic algorithms, and  
168 OPERA is trained and validated on curated PHYSPROP datasets.<sup>15, 38</sup> EPI Suite

169 primarily relies on fragment and bond contribution methods, which predicts compounds'  
170 overall properties by summing the properties of chemical fragments.<sup>13</sup> COSMOtherm,  
171 on the other hand, is based on the COSMO-RS (conductor-like screening model for real  
172 solvents) theory. This theory simulates surface charge density distribution on molecules  
173 to calculate intermolecular interactions, thereby predicting solubility, stability of  
174 coordination compounds, and other thermodynamic properties. SPARC utilizes  
175 computational algorithms grounded in the fundamental chemical structure theory to  
176 estimate a broad spectrum of physicochemical properties directly from molecular  
177 structure, enabling the prediction across diverse organic compounds and spanning  
178 chemical family boundaries.

179 The accuracy of each software application is sorted by the root-mean-square error  
180 (RMSE) and mean error (ME) calculated by the experimental values and the predicted  
181 values of physicochemical parameters of the chemicals in Group (1). The calculation  
182 methods of RMSE and ME are described in SI Text S4. Moreover, the applicability  
183 domains (ADs) of the *in silico* tools were considered to further evaluate the reliability  
184 of predictions, which could provide quantified criteria for identifying the optimal  
185 estimation strategy based on chemical structure and MWs.<sup>39, 40</sup> The ADs of the four *in*  
186 *silico* tools was introduced in the SI Text S5. Only the two QSAR models in our study  
187 have limited ADs. OPERA provides specific AD values for each substance to evaluate  
188 the prediction reliability, while EPI Suite provides specific training set database with  
189 applicable ranges of chemical MWs, structural fragment limits and measurements of  
190 parameters for individual modules (Tables S25-S27).<sup>15, 39, 41-45</sup> Chemicals falling

191 outside the EPI Suite estimation domain range were marked as “outside AD”, and  
192 considered low reliability (Table S10). Reliability scores were used to unify the  
193 different ADs forms provided by the two software applications (Tables S11-S12, S26-  
194 S27).<sup>15, 45</sup> COSMOtherm and SPARC have a broader chemical space, especially  
195 COSMOtherm, having an infinite AD.<sup>45</sup> It has to be clarified that the evaluation of  
196 predictions by all of RMSE, ME and ADs relies on experimental data, which have  
197 uncertainties due to operation and instrumentation errors, environmental influences or  
198 the systematic error and so on, even if standard laboratory methods are followed. This  
199 affects the prediction validation and probably will introduce uncertainties into our final  
200 estimation strategies. However, best attempts have been made to reduce the uncertainty  
201 in this study, and thus better qualified empirical data is still the best priority for  
202 prediction validation to date.

### 203 **Uncertainty evaluation.**

204 Precise knowledge of chemical multimedia distribution supports a better  
205 understanding of their environmental exposure routes, while persistence occupies a  
206 principal role in environmental risk assessment frameworks as the first criterion of the  
207 chemical PBT feature under the Stockholm Convention on Persistent Organic  
208 Pollutants.<sup>46</sup> Therefore, the SESAMe v3.4 model (Sino Evaluative Simplebox-MAMI  
209 model) was adopted to calculate the chemical multimedia distribution and overall  
210 persistence ( $P_{OV}$ ) of the 46 NOPEs, using different sets of physicochemical parameters  
211 predicted by the four *in silico* tools. How uncertainties in these parameters affect the  
212 environmental fate of the chemicals was assessed. SESAMe v3.4 is a well-developed

213 multimedia model having demonstrating good performance on organics with a broad  
214 range of properties, covering air, freshwater and sediment, seawater and sediment, soil  
215 (classified as natural, agricultural, and urban soil), and vegetation (natural and  
216 agricultural vegetation) compartments.<sup>10, 47-51</sup> The average values of environmental  
217 variables covering diverse climate zones in China were taken as input to the model for  
218 the simulation. The proportion of land use types included in the model was as follows:  
219 natural soil (80.2%), agricultural soil (17.1%), urban soil (1.7%), and freshwater (1.0%)  
220 (Table S13). The degradation half-lives input to the SESAMe v3.4 model were  
221 estimated by EPI Suite (Table S14). The modules used in EPI Suite for calculating  
222 degradation half-lives are specified in the SI Text S3. Uncertainties in half-life estimate  
223 are present, as (1) some substances are outside the training set of the EPI Suite BIOWIN  
224 and AOPWIN models, mainly used to estimate degradation half-lives in individual  
225 compartments, which reduces the reliability; and (2) the half-lives in soil and sediment  
226 are converted from the estimate for water by 1:2:9 ratio, which is a preliminary  
227 estimation method and also reduces the reliability of the estimation.<sup>13</sup> However, this is  
228 among the very few datasets/methods available to us, and will not affect the main  
229 research purpose of the study.

230 A theoretical emission was applied to all individual target compounds identically  
231 to compare the patterns of their multimedia distribution and  $P_{OV}$ . The proportion of  
232 emission to air, freshwater, and urban soil (86:11:3) was taken from the study by Chen  
233 et al. (2023), as limited information is available from existing studies.<sup>10</sup> The  $P_{OV}$  is the  
234 average time that a chemical resides in multiple environmental compartments, which

235 was calculated by the SESAMe v3.4 model based on Eq 3.<sup>52, 53</sup>

$$236 \quad P_{OV} = \frac{M_{total}}{E} \quad (3)$$

237 where  $E$  and  $M_{total}$  represent the emission rate (mol/day) and the total steady-state  
238 amount of a chemical (mol) in the system, respectively.<sup>54</sup>

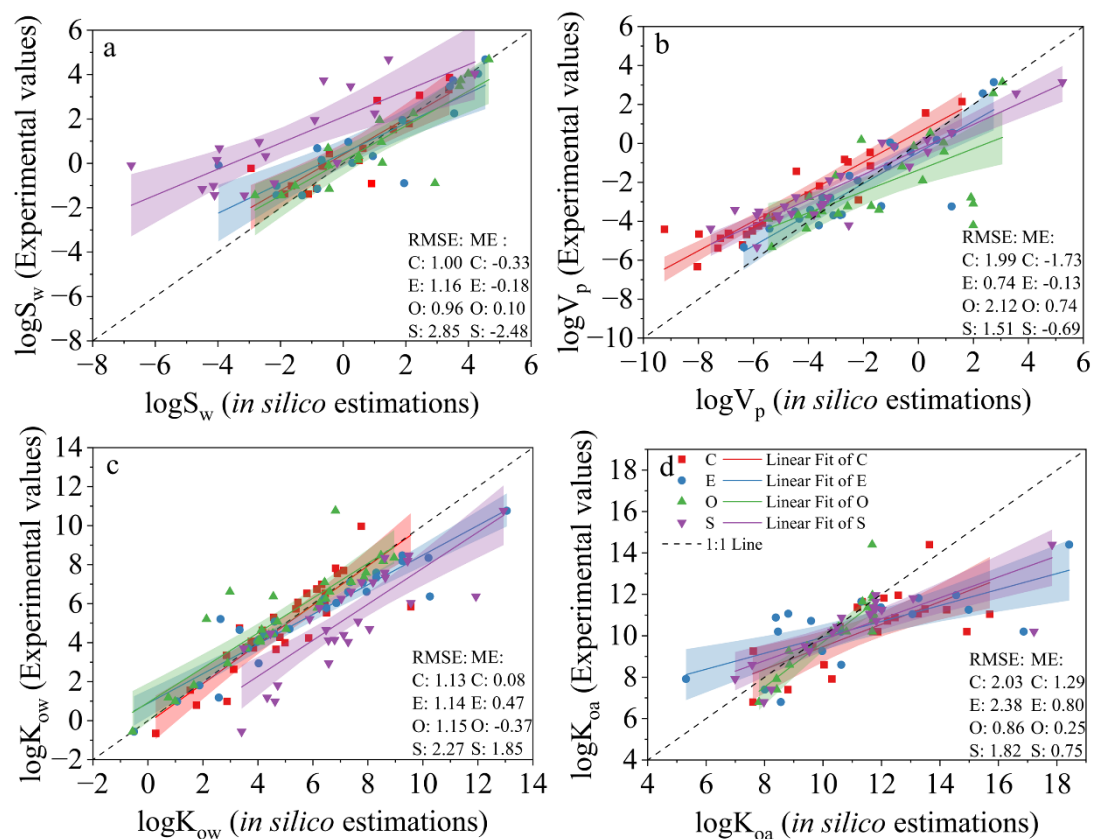
## 239 **Results and discussion**

### 240 **Comprehensive evaluation of software performance.**

241 The collected measured values of traditional FRs range from -1.38 to 3.87 (log  
242 mg/L) for  $\log S_w$ , -6.33 to 2.15 (log Pa) for  $\log V_p$ , -0.65 to 9.97 for  $\log K_{ow}$ , and 6.80 to  
243 14.4 for  $\log K_{oa}$ . Performance of the four software applications was mainly evaluated by  
244 comparing predictions (Tables S15-S18) with experimental data of the traditional FRs  
245 as stated above (Figures 2 and S2). The RMSE and ME reveal that none of the four  
246 software applications could consistently provide the most accurate estimates for all  
247 physicochemical properties of each substance (Figures 2 and S2). The same conclusion  
248 was also reached by Rodgers et al. (2021).<sup>21</sup> Overall, EPI Suite demonstrates better  
249 performance in predicting  $V_p$ , with a lower RMSE compared to the other three *in silico*  
250 tools (Figure 2a, b). COSMOtherm, EPI Suite and OPERA exhibit similar accuracy in  
251 predicting  $K_{ow}$  with RMSE values close to 1.13 log units. Additionally, OPERA  
252 provides predictions of  $S_w$  and  $K_{oa}$  with lower RMSE (0.96, 0.86 log units) and ME  
253 values (-0.10, 0.25 log units) than other *in silico* tools (Figure 2c, d).

254 However, the validation of OPERA predictions for  $K_{oa}$  of high-MW substances  
255 (e.g., 565 - 959 g/mol) may involve greater uncertainties compared to those for lower-  
256 MW substances. The predicted and measured  $\log K_{oa}$  values of PBDE 209 (MW, 959

257 g/mol) are 11.7 and 14.4, respectively, indicating a large discrepancy. Meanwhile, for  
258 the other high-MW substance with MWs rapidly increasing from 565 to 723 g/mol,  
259 both predicted and measured  $K_{oa}$  values fall within an extremely narrow range from 11.7  
260 to 12.0 and from 11.4 to 11.7, respectively (Tables S8 and S18). A similar issue is  
261 observed in predictions for NOPEs. This is unreasonable, indicating failure of accurate  
262 prediction and measurement. High-MW chemicals, with extremely low volatility ( $\log$   
263  $K_{oa} > 12$ ), will have a negligible amount partitioning into the air phase during  
264 equilibrium partitioning experiments, which more likely result in inaccurate  
265 measurement of air concentrations and consequently the  $K_{oa}$ , probably due to proximity  
266 to the instrument's detection limit. For less volatile chemicals,  $K_{oa}$  is also hardly reliably  
267 measured, as kinetic limitations may inhibit the phase equilibrium being reached.<sup>35</sup> For  
268 predictions, only 78% of the high-MW substances are inside the ADs of OPERA for  
269  $K_{oa}$  prediction, which is lower than the percentage of 96% for lower-MW substances  
270 (Table S27). The reliability of predictions decreases for chemicals outside the ADs.  
271 Meanwhile, OPERA gives similar predictions when targeted chemicals have similar  
272 structures. Many high-MW FRs are PBDE congeners with a similar structure, which  
273 may result in the close  $K_{oa}$  predictions.



274

275 **Figure 2.** Comparison of the *in silico* estimates and experimental values of the  
 276 traditional FRs to evaluate the performance of different *in silico* tools. The dashed lines  
 277 represent the 1:1 agreement; the solid lines show the regressions between the measured  
 278 and the simulated data; the shaded areas represent the 95% confidence interval of the  
 279 regression. C, E, O and S represent the COSMOtherm, EPI Suite, OPERA and SPARC  
 280 model, respectively. RMSE indicates root-mean-square error, ME indicates mean error.  
 281 RMSE and ME are in logarithmic units.

282 More specifically, for individual categories of BFRs, alkyl-OPEs, aryl-OPEs, and  
 283 halogenated-OPEs, the four *in silico* tools show varying uncertainties. COSMOtherm  
 284 and OPERA perform significantly better (RMSE, 0.27–2.29 log units) than the other  
 285 two software applications (RMSE, 0.36–4.50 log units) in predicting  $S_w$  for all  
 286 categories (Figure S2a-d). Meanwhile, COSMOtherm also demonstrates the best

287 performance in predicting  $K_{ow}$  of BFRs; and it generally has a strong performance on  
288  $K_{ow}$  for all OPEs. Although it does not rank the top two on most occasions, the  
289 difference from the superior software was minimal. EPI Suite has the best performance  
290 on  $V_p$  for all categories,  $S_w$  for halogenated-OPEs and  $K_{ow}$  for alkyl-OPEs; and it is one  
291 of the top two *in silico* tools in estimating  $S_w$  and  $K_{ow}$  of BFRs (inferior to  
292 COSMOtherm) and aryl-OPEs (inferior to OPERA). OPERA exhibits the best accuracy  
293 for predicting  $K_{ow}$  for aryl-OPEs and halogenated-OPEs,  $K_{oa}$  for alkyl-OPEs and  
294 halogenated-FRs, including BFRs and halogenated-OPEs, and  $V_p$  for BFRs. It ranks  
295 second in predicting  $K_{ow}$  of alkyl-OPEs (inferior to EPI Suite) and  $K_{oa}$  of aryl-OPEs  
296 (inferior to SPARC), but the difference from the top-ranked software is not significant.  
297 SPARC was the best for predicting  $K_{oa}$  of aryl-OPEs (Figure S2) and ranked the second  
298 for predicting  $V_p$  of OPEs. The rank of software performance based on RMSE is  
299 provided in Table S19.

300       However, the uncertainty of predictions increases with growing MWs and  
301 structure complexity for all software applications, although to varying extents. As  
302 shown in Figure S2, the predictions exhibit a greater discrepancy from the measurement  
303 for chemicals with higher MWs across nearly all four parameters, which is illustrated  
304 by the increasing deviation of data points from the 1:1 line for higher-MW chemicals.  
305 As the MW or structural complexity of a substance increases, it typically comprises a  
306 greater number of or more intricate structural fragments. A higher percentage of these  
307 substances are outside the ADs or training set of the two QSAR models, compared to  
308 those with lower MWs. Even if they fall within the ADs, they are generally associated

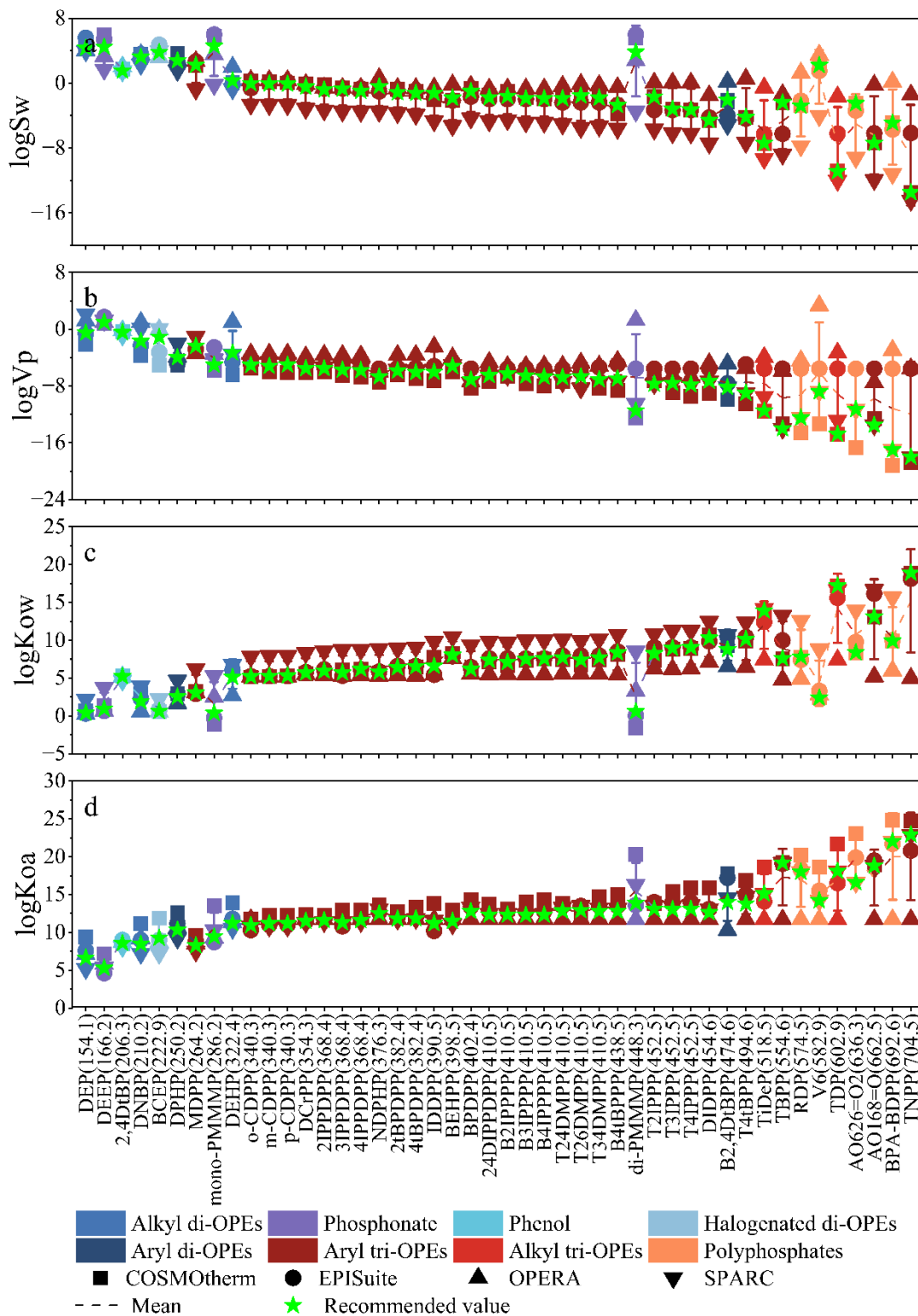


309 with “Caution advised” or “unreliable” reliability scores (Tables S26 and S27). By  
310 comparing RMSEs, the QSAR model’s predictions for substances outside the training  
311 set have reduced accuracy compared to the substances within the training set (Tables  
312 S28 and S29). For example, the RMSEs of the  $\log V_p$  for substances inside and outside  
313 the training set of the MPBVP module of the EPI Suite model are 0.75 and 1.77 log  
314 units, respectively. This was also observed by Zhang et al. (2016), who reported larger  
315 discrepancies in model estimates for novel FRs with MWs exceeding 800 g/mol, which  
316 were largely attributed to the models’ reliance on training sets composed of lower MW  
317 compounds.<sup>55</sup> Wang et al. (2017) also found similar trends when predicting gas-aqueous  
318 partitioning for volatile organic compounds with different number of functional groups  
319 and MWs.<sup>56</sup>

### 320 **Estimated physicochemical properties of NOPEs.**

321 Although each *in silico* tool shows advantages in predicting at least one variable  
322 for traditional FRs, EPI Suite and OPERA presented limitations on NOPEs owing to  
323 their operational principle based on empirical data. Figure 3 shows that when MWs of  
324 tri-OPEs and polyphosphate esters increased from 453 to 705 g/mol, OPERA generates  
325 very narrow ranges from -6.5 to -5.6 (log Pa) for  $\log V_p$ , from -1.52 to 0.53 (log mg/L)  
326 for  $\log S_w$ , and from 4.8 to 7.14 for  $\log K_{ow}$ , while the predicted  $\log K_{oa}$  is even stable at  
327 around 11.7. Similarly, the estimation of  $\log V_p$  by EPI Suite ranges only from -5.6 to -  
328 4.9 (log Pa). The same phenomenon was observed in a previous study when estimating  
329  $\log K_{aw}$  of PFAS by OPERA.<sup>18</sup> This is due to the use of the nearest neighbor algorithm  
330 and the lack of experimental data of chemicals with high MWs in the training set. There

331 is no measurement data used in the training set due to the challenge of accurately  
332 measuring phase distributions when the chemicals predominantly distribute in one  
333 phase. For instance, if a chemical has a  $K_{oa}$  value exceeding  $10^{12}$ , its transfer from the  
334 octanol phase to the air phase would become too small to be measured. As a fragment-  
335 based model, the bias of EPI Suite increases with the enlarged chemical structural  
336 complexity, due to the aggregate of small errors induced by growing numbers and  
337 complexity of bond fragments.<sup>57</sup> Ebert et al. noticed the same phenomenon for  $K_{aw}$   
338 prediction using EPI Suite HENRYWIN.<sup>57</sup> Consequently, these two *in silico* tools may  
339 face inherent limitations in providing reliable estimates of the four parameters,  
340 especially for the NOPEs with larger MWs and complex structures that fall outside  
341 existing database of the software.



342

343 **Figure 3.** Predicted values, mean, standard deviation and recommended values of  $\log V_p$ ,

344  $\log S_w$ ,  $\log K_{ow}$  and  $\log K_{oa}$  for NOPEs. The values in parentheses represent the molecular

345 weights of the substances.

346 In contrast, COSMOtherm and SPARC are based on quantum chemical principles  
347 and fundamental chemical structure theory, respectively. Predictions of chemicals with  
348 high MWs using the two approaches show a more reasonable changing pattern.<sup>58-60</sup> As  
349 the complexity of the molecular structure increases, both COSMOtherm and SPARC  
350 can better predict significant changes in physicochemical parameters, more accurately  
351 reflecting the large differences between compounds with higher and lower MWs, as has  
352 been observed in previous studies.<sup>55</sup> For example, for tri-OPEs and polyphosphate  
353 esters with MWs ranging from 453 to 705 g/mol, the estimates of  $\log V_p$ ,  $\log S_w$ ,  $\log K_{ow}$   
354 and  $\log K_{oa}$  span from -7 to -19 (log Pa), -1.7 to -14.5 (log mg/L), 7.39 to 18.9, and 13.1  
355 to 24.8, respectively, exhibiting considerably larger variations compared to those  
356 predicted by EPI Suite and OPERA (Figure 3 and Tables S20-S23). Therefore,  
357 significant discrepancies in predictions over 3 log units are observed among the four *in*  
358 *silico* tools when MWs exceeded 450 g/mol for  $S_w$  and  $V_p$ , and 500 g/mol for  $K_{ow}$  and  
359  $K_{oa}$ . Zhang et al. also found large discrepancies among model predictions with rising  
360 MWs, which could even reach 12 log units for chemicals having MWs >800 g/mol.<sup>55</sup>  
361 Meanwhile, based on reliability score, it is also found that 450 g/mol and 500 g/mol are  
362 proper thresholds, as a greater number of NOPEs with MWs higher than the two  
363 thresholds fall outside the ADs for individual parameters than NOPEs with MWs lower  
364 than the thresholds. This indicates reduced reliability of the two QSAR models in  
365 prediction for the high-MWs substances. This reflects that making predictions for high-  
366 molecular-weight compounds should be done extremely cautiously. However, some  
367 predictions still need to be made—even though they have high uncertainty—to fulfill

368 the research objectives on these compounds.

369 In this case, by comprehensively considering the rank obtained by the software  
370 evaluation on traditional FRs, software performance on NOPEs and operational  
371 principles, this study recommends varying optimal *in silico* tools to predict the four  
372 physicochemical parameters of novel substances with different MWs, using 450 g/mol  
373 and 500 g/mol as thresholds. Given the small difference between the *in silico* tools when  
374 MWs are below these thresholds, the average value is taken from the top three *in silico*  
375 tools for all parameters. The software is ranked based on RMSE derived from validation  
376 on traditional FRs (Table S19). For NOPEs with MWs above the thresholds, the first-  
377 ranked non-QSAR software is used for individual parameters, considering the reduced  
378 reliability of QSAR models on these high-MW chemicals as discussed above. For  
379 compounds with MWs greater than 450 g/mol, COSMOtherm and SPARC are preferred  
380 for  $S_w$  and  $V_p$  respectively for all substance categories. For all compounds with MWs  
381 exceeding 500g/mol, COSMOtherm and SPARC are recommended to predict  $K_{ow}$  and  
382  $K_{oa}$ , respectively (Table 1). The recommended values of the four physicochemical  
383 parameters for NOPEs are provided in Table S1. However, limited empirical data may  
384 introduce uncertainties into the verification and thus the recommendation, which  
385 requires more experimental data for confirmation or calibration. But the recommended  
386 values have been the most reasonable and reliable based on current available tools and  
387 methods.

388 **Table 1.** Recommended software predictions for OPEs with molecular weights

389 (MWs) >450/500 g/mol.

<b>Compounds</b>	<b>S<sub>w</sub></b> (>450 g/mol)	<b>V<sub>p</sub></b> (>450 g/mol)	<b>K<sub>ow</sub></b> (>500 g/mol)	<b>K<sub>oa</sub></b> (>500 g/mol)
Alkyl-OPEs	COSMOtherm	SPARC	COSMOtherm	SPARC
Aryl-OPEs	COSMOtherm	SPARC	COSMOtherm	SPARC
Halogenated-OPEs	COSMOtherm	SPARC	COSMOtherm	SPARC

390 For all categories, logS<sub>w</sub> and logV<sub>p</sub> generally decrease when the number of carbon  
391 atoms increases, with logS<sub>w</sub> ranging from -13.5 to 5.1 (log mg/L) and logV<sub>p</sub> from -18.0  
392 to 1.3 (log Pa). In contrast, logK<sub>ow</sub> and logK<sub>oa</sub> exhibit an increasing trend with growing  
393 carbon atoms, with logK<sub>ow</sub> ranging from 0.4 to 18.9 and logK<sub>oa</sub> from 5.3 to 22.9 (Figure  
394 3 and Table S1). This suggests that the hydrophobicity of the compounds increases with  
395 the addition of carbon atoms, while the volatility progressively decreases. For  
396 chemicals with the same number of carbon atoms, different functional groups  
397 effectively influence chemical properties. The alkyl-OPEs, having the same number of  
398 carbon atoms as aryl-OPEs, exhibit lower water solubility and higher log K<sub>ow</sub> than  
399 corresponding aryl-OPEs, indicating stronger lipophilicity. For example, TiDeP and  
400 TDP, as alkyl-OPEs, have a logS<sub>w</sub> at -7.4 and -10.9 (log mg/L), respectively, and logK<sub>ow</sub>  
401 at 13.9 and 17.2 (Table S1); while T4tBPP and TBPP, as two aryl-OPEs having the same  
402 number of carbon atoms with the above two alkyl-OPEs, present a higher logS<sub>w</sub> at -4.2  
403 and -2.4 (log mg/L), and lower logK<sub>ow</sub> values at 8.9 and 7.6, respectively (Table S1).  
404 Moreover, an increase in phosphate groups enhances molecular polarity by facilitating  
405 hydrogen bond formation when the number of carbon atoms remains the same, thereby  
406 increasing the water solubility of the chemicals.<sup>61</sup> For instance, both as aryl-OPEs

407 having an identical carbon atom count, RDP possessing an additional phosphate group  
408 than T4tBPP has a greater  $\log S_w$  (-2.8 versus -4.2, log mg/L) and a lower  $\log K_{ow}$  (7.8  
409 versus 8.9) than T4tBPP. Chlorine substituents also play a critical role in enhancing the  
410 water solubility of chemicals by amplifying polar interactions. For example, V6, which  
411 contains six chlorine atoms, shows higher water solubility with a  $\log S_w$  value of 2.2  
412 (log mg/L). In addition to chlorination, oxidation reactions—particularly the addition  
413 of hydroxyl groups—can greatly increase the hydrophilicity of transformation products  
414 compared to their parent tri-OPEs. This rise in polarity is evidenced by higher  $\log S_w$   
415 values and lower  $\log K_{ow}$  values (Figure S1). A typical example is BCEP, a  
416 transformation product of TCEP, which forms through photooxidation reactions, as  
417 reported by Liu et al (2021).<sup>8</sup> BCEP exhibits a lower  $\log K_{ow}$  of 0.64 compared to 1.57  
418 for TCEP (Figure S1), further highlighting how oxidative processes enhance both  
419 solubility and polarity.

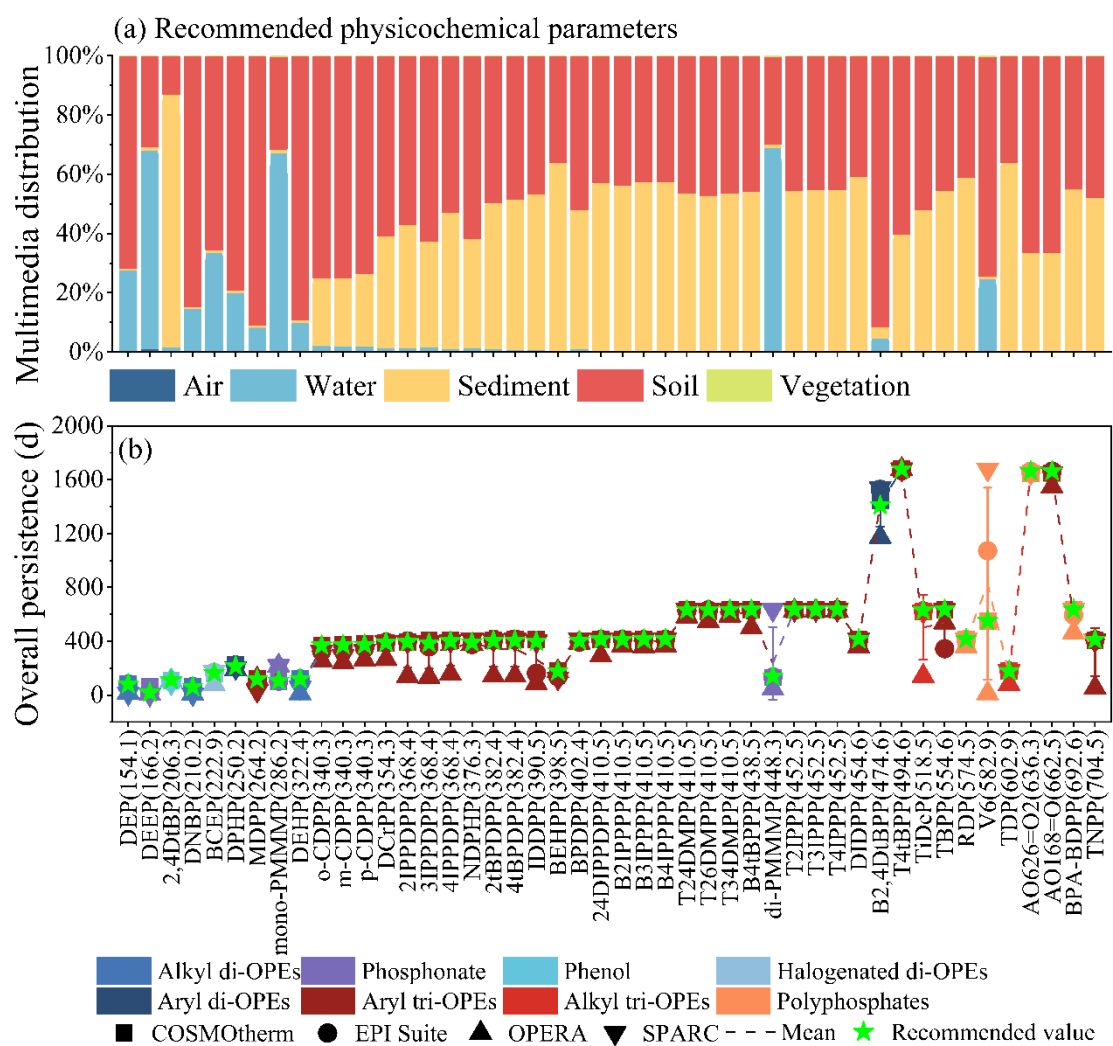
420 **Impact of uncertainty in physicochemical parameters on predicting multimedia**  
421 **distribution.**

422 All four *in silico* tools provide physicochemical parameters indicating negligible  
423 distribution in the air for all NOPEs under both equilibrium conditions (Figure S3) and  
424 the steady state (Figure 4a). The difference of the two conditions is described in SI Text  
425 S6. However, equilibrium partitioning illustrated by  $K_{ow}$  and  $K_{aw}$  in Figure S3 shows  
426 that predictions by COSMOtherm and EPI Suite lead to greater variability in chemical  
427 partitioning between water and solid phases (sediment/soil) at equilibrium than those  
428 from the other software applications. The prediction by SPARC also suggests a

429 relatively variable partitioning but indicates a greater tendency for substances to  
430 distribute in air compared to the other software applications. In contrast, OPERA  
431 generates the most consistent partitioning of the NOPEs at equilibrium, with slightly  
432 higher partitioning in the water phase compared to other phases (Figure S3).

433       Steady-state distributions predicted by the SESAMe v3.4 model reveal that, with  
434 the input of recommended physicochemical parameters, despite 86% of emissions  
435 entering the atmosphere, novel tri-OPEs and polyphosphate esters are primarily  
436 distributed in sediments (23–64%) and soils (36–75%), together accounting for over  
437 98% of the total mass remaining in the multimedia system (Figure 4a). As MWs  
438 increase, the distribution shifts, showing an increasing proportion in sediment  
439 compared to soil. Furthermore, V6, a halogenated-polyphosphate ester, shows the  
440 highest percentage in the water compartment (25%) among all polyphosphate esters, as  
441 a result of its highest water solubility and long half-life in water (Figure 4a and Table  
442 S14).





443

444 **Figure 4.** (a) Multimedia environmental distribution of NOPEs under steady state  
 445 predicted by the SESAME v3.4 model with inputs of recommended physicochemical  
 446 parameter values; (b) Overall persistence predicted by the SESAME v3.4 model, with  
 447 input of recommended physicochemical parameter values and predictions by individual  
 448 *in silico* tools. The values in parentheses represent the molecular weights of the  
 449 substances.

450 Novel di-OPEs are generally more hydrophilic than their parent compounds, as  
 451 indicated by higher  $S_w$  and lower  $K_{ow}$  values, causing a greater distribution in the water  
 452 compartment (Figure 4a). As a special case, the phenolic transformation product of

453 AO168=O, i.e., 2,4DtBP, is mainly distributed in the sediment (85%)—the highest  
454 distribution in the sediment compartment of all NOPEs. This is because of its moderate  
455 water solubility ( $\log S_w$  at 1.77, log mg/L) and  $\log K_{ow}$  (5.23), which makes 2,4-DtBP  
456 more likely to partition in the soluble phase of the soil pore water than other NOPEs,  
457 and be transported to freshwater systems by surface land runoff. Meanwhile, 2,4-DtBP  
458 is more easily distributed in the sediment than other novel di-OPEs. The three  
459 phosphonate esters, namely DEEP, mono-PMMMP and di-PMMMP, are primarily  
460 distributed in water and soil compartments, with 67%, 67% and 69% in water, and 31%,  
461 31% and 30% in soil, respectively (Figure 4a). DEEP exhibits a slightly higher  
462 distribution in air (1.2%) compared to other phosphonate esters because of its much  
463 higher  $\log V_p$  and lower  $\log K_{oa}$  (Figure 4a), while other phosphonate esters and even all  
464 other novel tri-OPEs have a  $\log V_p < 0$  and  $\log K_{oa} > 5.5$ .

465       Uncertainties are shown in the multimedia distribution simulated by taking the  
466 non-recommended values for physicochemical parameters (i.e.  $S_w$ ,  $V_p$ , and  $K_{ow}$ )  
467 provided by the different software applications, compared to those using recommended  
468 values. The most pronounced uncertainties concentrate on soil and sediment  
469 distribution for low-molecular-weight (<360 g/mol) and high-molecular-weight OPEs  
470 (>600 g/mol), reaching up to 83%. COSMOtherm and EPI Suite provide a closer  
471 distribution pattern in sediment (0.5–86%), soil (12–92%), and water (0.1–75%) to that  
472 calculated by the recommended values for chemicals with MWs below 450 g/mol  
473 (Figures 4a and S4a, b). However, when using SPARC, the deviation from using  
474 recommended values is the greatest for the low-molecular-weight chemicals (<360

475 g/mol) (Figures 4a and S4d). Specifically, adopting SPARC tends to result in a deviation  
476 in water distribution by up to 65% (mono-PMMMP), and in sediment and soil  
477 distribution by 83% and 77%, respectively (MDPP). For chemicals with MWs between  
478 400 and 450 g/mol, OPERA would underestimate the distribution in sediments by up  
479 to 22% and overestimate the distribution in soil by up to 37% (Figures 4a and S4c). For  
480 chemicals with MWs >600 g/mol, particularly AO168=O, AO626=O<sub>2</sub>, and TNPP, the  
481 physicochemical parameters predicted by single software alone cannot obtain  
482 reasonable multimedia distributions, with the sediment and soil distributions differing  
483 from the recommendations by up to 47%. Furthermore, only using the physicochemical  
484 parameters predicted by recommended software like COSMOtherm or SPARC also  
485 result in significant inaccuracies in multimedia distributions, e.g. the sediment and soil  
486 distribution deviation of TiDeP (MW >500 g/mol) is up to 43%.

487 **Impacts of uncertainty in physicochemical parameters on predicting overall**  
488 **persistence.**

489 High persistence indicates the potential for prolonged environmental and human  
490 exposure to a substance, which is difficult to control or remove. As indicated above, it  
491 has been suggested as a highly concerned chemical inherent feature on its own. By  
492 inputting the recommended values of physicochemical parameters, T4tBPP, AO168=O,  
493 AO626=O<sub>2</sub> and B2,4DtBPP display the highest P<sub>OV</sub> of the tested chemicals, ranging  
494 from ~4–4.6 years, longer than the P<sub>OV</sub> of the other target NOPEs (18 days ~ 1.7 years)  
495 (Figure 4b). This is primarily attributed to their predominant distribution in soil  
496 (60–91%) and sediment (4–40%), accounting for over 95% of the total remaining mass,

497 and their long half-lives in soil (360 days) and sediment (4.4 years) (Table S14). These  
498 four substances could be classified as “very persistent” (vP) under the EU REACH  
499 criterion, which requires a residence time exceeding 60 days in water, 180 days in soil,  
500 and 540 days in sediment.<sup>62</sup>

501  $P_{OV}$  of other novel tri-OPEs and polyphosphate esters (from 118 days to 1.7 years)  
502 is less than that of the aforementioned four substances, with MDPP, BEHPP and TDP  
503 exhibiting the lowest  $P_{OV}$  (<179 days). Under steady state, MDPP is mainly distributed  
504 in soil (91%), with additional 8% in water and 1% in sediment, while both BEHPP and  
505 TDP are predominantly distributed in sediment (64%) and soil (36%). These half-lives  
506 of these three chemicals in the key environmental compartments are the lowest among  
507 all the target compounds (Table S14). It is the reason why they have the lowest  $P_{OV}$ .  
508 Novel di-OPEs generally have lower  $P_{OV}$  (61–214 days, except for B2,4DtBPP) than  
509 the selected novel tri-OPEs (Figure 4b). However, most of them (DPHP, MDPP, DEP,  
510 DNBP and BCEP) demonstrate  $P_{OV}$  2 to 16 times higher than their precursors (Figure  
511 S5a, c-f). Only B2,4DtBPP and 2,4DtBP are less persistent than their precursor  
512 AO168=O (Figure S5b). The  $P_{OV}$  of the three phosphonate esters ranges from 18 to 140  
513 days (Figure 4b).

514 If using only one software tool, COSMOtherm could yield  $P_{OV}$  estimates closer to  
515 the recommended values for novel tri-OPEs and polyphosphate esters, while SPARC  
516 may overestimate the  $P_{OV}$  of these substances by up to 3 years (V6) and other two tools  
517 may underestimate the  $P_{OV}$  by up to 1.5 years. For novel di-OPEs and phosphonate  
518 esters, the deviations caused by using OPERA and SPARC can exceed 1 year. Overall,

519 using single software can result in  $P_{OV}$  deviations ranging 0–350%, and generates the  
520 highest uncertainty on  $P_{OV}$  estimates for di-PMMMP, TiDeP, TNPP and V6, with  
521 deviations of 1 to 3 years. The overestimation by SPARC for di-PMMMP is primarily  
522 because it overpredicted the diffusive mass flux from water to sediment and  
523 sedimentation, combined with an underestimation of soil runoff and sediment  
524 resuspension. This increases the mass retained in sediment and soil, consequently,  
525 overall persistence. In contrast, OPERA underestimates TiDeP and TNPP for the  
526 opposite reason. Using single software could result in the largest deviation of retained  
527 mass in soils and sediments at the steady state for V6, compared to other substances,  
528 resulting in the high deviation of  $P_{OV}$  for V6.

### 529 **Perspectives.**

530 This research provides the first and most reliable reference values for essential  
531 physicochemical parameters of 46 NOPEs, covering a wide variety of MWs and  
532 structures. These reference values are valuable because the property ranges of the  
533 NOPEs made direct measurement of the physicochemical properties infeasible. The  
534 discussion on impact of uncertainties in physicochemical parameters on predicting  
535 multimedia distribution and  $P_{OV}$  has revealed potential deviations when using different  
536 software to predict these parameters and highlighted the characteristics of  
537 environmental behavior of these novel compounds. Reliable knowledge of chemical  
538 properties is the premise of accurate understanding of environmental behaviors,  
539 exposure routes and risks of chemicals, as well as efficient management of chemical  
540 use and contamination. This study has filled data gaps and provided solutions regarding

541 defects of the existing software in predicting physicochemical properties, which could  
542 be further applied to other emerging contaminants. However, it should be noted that the  
543 MW thresholds for prediction were established based on the evaluation of the targeted  
544 FRs and NOPEs in this study. Further evaluation across broader chemical categories  
545 may be needed to validate these thresholds in future work when expanding the strategy  
546 application on other chemicals.

547 Future research should fully leverage the powerful computational capabilities of  
548 modern computers, particularly machine learning and artificial intelligence  
549 technologies, to further develop methods based on COSMO-RS and fundamental  
550 chemical structure theory.<sup>63, 64</sup> By integrating machine learning models with existing  
551 algorithms for molecular surface charge density distribution and molecular structure  
552 deduction, deeper insights can be achieved into the interactions between atoms,  
553 electrons, and functional groups, thereby improving the accuracy of chemical property  
554 predictions. These methods hold even greater potential in cases where prior data is  
555 lacking or for complex structures which are not present in databases. Meanwhile, more  
556 attention should focus on building larger training datasets and developing multi-scale  
557 computational models to more accurately predict the physicochemical properties of  
558 organic compounds with more complex structure under various conditions, thereby  
559 advancing fields such as materials science, chemical engineering, environmental  
560 science and public health etc. As global concerns about chemical safety grow, this study  
561 underscores the critical role of advanced computational tools in filling data gaps and  
562 mitigating the risks associated with emerging contaminants.

563 **Associated content**

564 **Supporting Information**

565 The Supporting Information is available at <https://pubs.acs.org>

566 The information, structure, application and recommended physicochemical  
567 properties of the target NOPEs; the information of traditional FRs; SMILES strings for  
568 NOPEs and traditional FRs; data for experimental and estimated physicochemical  
569 parameters of traditional FRs; EPI Suite model selection; plot of comparison of *in silico*  
570 estimates and experimental data of physicochemical parameters for traditional FRs;  
571 software performance rankings; application domains and reliability evaluations for  
572 QSAR models; RMSE and ME for various validated substances; estimates of  
573 physicochemical parameters of NOPEs by the four *in silico* tools; parameters input into  
574 the SESAMe v3.4 model; degradation half-lives for NOPEs; chemical structure and  
575 overall persistence for OPEs and corresponding transformation products; plots of  
576 equilibrium partitioning characteristics and multimedia environmental distributions  
577 based on estimated physicochemical parameters of NOPEs.

578 **Acknowledgement**

579 This study is supported by the by the National Natural Science Foundation of  
580 China (42377362, 423B1003 and 72088101), the Research Start-up Funding from  
581 Shanghai Jiao Tong University and the Shanghai Oriental Talent Program - Youth  
582 Project.

583 **Reference**

- 584 1. van der Veen I, de Boer J. Phosphorus flame retardants: Properties, production,  
585 environmental occurrence, toxicity and analysis. *Chemosphere*, **2012**, 88 (10):

- 586 1119-1153.
- 587 2. Xie Z, Wang P, Wang X, Castro-Jiménez J, Kallenborn R, Liao C, Mi W, Lohmann  
588 R, Vila-Costa M, Dachs J. Organophosphate ester pollution in the oceans. *Nature*  
589 *Reviews Earth & Environment*, **2022**, 3 (5): 309-322.
- 590 3. Zhu H, Al-Bazi M M, Kumosani T A, Kannan K. Occurrence and Profiles of  
591 Organophosphate Esters in Infant Clothing and Raw Textiles Collected from the  
592 United States. *Environmental Science & Technology Letters*, **2020**, 7 (6): 415-420.
- 593 4. Sühling R, Diamond M L, Bernstein S, Adams J K, Schuster J K, Fernie K, Elliott  
594 K, Stern G, Jantunen L M. Organophosphate Esters in the Canadian Arctic Ocean.  
595 *Environmental Science & Technology*, **2021**, 55 (1): 304-312.
- 596 5. Gu L, Hu B, Fu Y, Zhou W, Li X, Huang K, Zhang Q, Fu J, Zhang H, Zhang A, Fu  
597 J, Jiang G. Occurrence and risk assessment of organophosphate esters in global  
598 aquatic products. *Water Research*, **2023**, 240: 120083.
- 599 6. Tian Y X, Chen H Y, Ma J, Liu Q Y, Qu Y J, Zhao W H. A critical review on sources  
600 and environmental behavior of organophosphorus flame retardants in the soil:  
601 Current knowledge and future perspectives. *Journal of Hazardous Materials*, **2023**,  
602 452: 131161.
- 603 7. Blum A, Behl M, Birnbaum L S, Diamond M L, Phillips A, Singla V, Sipes N S,  
604 Stapleton H M, Venier M. Organophosphate Ester Flame Retardants: Are They a  
605 Regrettable Substitution for Polybrominated Diphenyl Ethers? *Environmental*  
606 *Science & Technology Letters*, **2019**, 6 (11): 638-649.
- 607 8. Liu Q, Li L, Zhang X, Saini A, Li W, Hung H, Hao C, Li K, Lee P, Wentzell J J B,  
608 Huo C, Li S M, Harner T, Liggio J. Uncovering global-scale risks from commercial  
609 chemicals in air. *Nature*, **2021**, 600 (7889): 456-461.
- 610 9. Liu Q, Liu R, Zhang X, Li W, Harner T, Saini A, Liu H, Yue F, Zeng L, Zhu Y,  
611 Xing C, Li L, Lee P, Tong S, Wang W, Ge M, Wang J, Wu X, Johannessen C,  
612 Liggio J, Li S-M, Hung H, Xie Z, Mabury S A, Abbatt J P D. Oxidation of  
613 commercial antioxidants is driving increasing atmospheric abundance of  
614 organophosphate esters: Implication for global regulation. *One Earth*, **2023**, 6 (9):  
615 1202-1212.
- 616 10. Chen R, Xing C, Shen G, Jones K C, Zhu Y. Indirect Emissions from  
617 Organophosphite Antioxidants Result in Significant Organophosphate Ester  
618 Contamination in China. *Environmental Science & Technology*, **2023**, 57 (48):  
619 20304-20314.
- 620 11. Sühling R, Wolschke H, Diamond M L, Jantunen L M, Scheringer M. Distribution  
621 of Organophosphate Esters between the Gas and Particle Phase—Model Predictions  
622 vs Measured Data. *Environmental Science & Technology*, **2016**, 50 (13): 6644-  
623 6651.
- 624 12. BIOVIA, BIOVIA COSMOtherm 2021, version 21.0. Dassault Systèmes: 2021.  
625 <https://www.3ds.com/products/biovia/cosmo-rs/cosmotherm> (accessed 2023-07-  
626 15).
- 627 13. U.S. EPA, Estimation Programs Interface Suite for Microsoft Windows (EPI Suite  
628 v4.11). U.S. Environmental Protection Agency: 2023. (accessed 2023-08-10).
- 629 14. ArChemCalc, SPARC Performs Automated Reasoning in Chemistry (SPARC).



- 630 ArChemCalc: 2024. <http://archemcalc.com/sparc-web/calc> (accessed 2023-08-02).
- 631 15. Mansouri K, Grulke C M, Judson R S, Williams A J. OPERA models for predicting  
632 physicochemical properties and environmental fate endpoints. *Journal of*  
633 *Cheminformatics*, **2018**, 10 (1): 10.
- 634 16. Stenzel A, Goss K-U, Endo S. Prediction of partition coefficients for complex  
635 environmental contaminants: Validation of COSMOtherm, ABSOLV, and SPARC.  
636 *Environmental Toxicology and Chemistry*, **2014**, 33 (7): 1537-1543.
- 637 17. Endo S. Intermolecular Interactions, Solute Descriptors, and Partition Properties  
638 of Neutral Per- and Polyfluoroalkyl Substances (PFAS). *Environmental Science &*  
639 *Technology*, **2023**, 57 (45): 17534-17541.
- 640 18. Endo S, Hammer J, Matsuzawa S. Experimental Determination of Air/Water  
641 Partition Coefficients for 21 Per- and Polyfluoroalkyl Substances Reveals Variable  
642 Performance of Property Prediction Models. *Environmental Science & Technology*,  
643 **2023**, 57 (22): 8406-8413.
- 644 19. Gomis M I, Wang Z, Scheringer M, Cousins I T. A modeling assessment of the  
645 physicochemical properties and environmental fate of emerging and novel per- and  
646 polyfluoroalkyl substances. *Science of The Total Environment*, **2015**, 505: 981-991.
- 647 20. Wang Z, MacLeod M, Cousins I T, Scheringer M, Hungerbühler K. Using  
648 COSMOtherm to predict physicochemical properties of poly- and perfluorinated  
649 alkyl substances (PFASs). *Environmental Chemistry*, **2011**, 8 (4): 389-398.
- 650 21. Rodgers T F M, Okeme J O, Parnis J M, Girdhari K, Bidleman T F, Wan Y,  
651 Jantunen L M, Diamond M L. Novel Bayesian Method to Derive Final Adjusted  
652 Values of Physicochemical Properties: Application to 74 Compounds.  
653 *Environmental Science & Technology*, **2021**, 55 (18): 12302-12316.
- 654 22. Hammer J, Endo S. Volatility and Nonspecific van der Waals Interaction Properties  
655 of Per- and Polyfluoroalkyl Substances (PFAS): Evaluation Using Hexadecane/Air  
656 Partition Coefficients. *Environmental Science & Technology*, **2022**, 56 (22):  
657 15737-15745.
- 658 23. Kuramochi H, Takigami H, Scheringer M, Sakai S-i. Estimation of  
659 physicochemical properties of 52 non-PBDE brominated flame retardants and  
660 evaluation of their overall persistence and long-range transport potential. *Science*  
661 *of The Total Environment*, **2014**, 491-492: 108-117.
- 662 24. Zhang X, Brown T N, Wania F, Heimstad E S, Goss K-U. Assessment of chemical  
663 screening outcomes based on different partitioning property estimation methods.  
664 *Environment International*, **2010**, 36 (6): 514-520.
- 665 25. Tan H, Chen D, Peng C, Liu X, Wu Y, Li X, Du R, Wang B, Guo Y, Zeng E Y.  
666 Novel and Traditional Organophosphate Esters in House Dust from South China:  
667 Association with Hand Wipes and Exposure Estimation. *Environmental Science &*  
668 *Technology*, **2018**, 52 (19): 11017-11026.
- 669 26. Liu R, Mabury S A. Organophosphite Antioxidants in Indoor Dust Represent an  
670 Indirect Source of Organophosphate Esters. *Environmental Science & Technology*,  
671 **2019**, 53 (4): 1805-1811.
- 672 27. Kutarna S, Chen W, Xiong Y, Liu R, Gong Y, Peng H. Screening of Indoor  
673 Transformation Products of Organophosphates and Organophosphites with an in

- 674 Silico Spectral Database. *ACS Measurement Science Au*, **2023**, 3 (6): 469-478.
- 675 28. Hu J, Lyu Y, Li M, Wang L, Jiang Y, Sun W. Discovering Novel Organophosphorus  
676 Compounds in Wastewater Treatment Plant Effluents through Suspect Screening  
677 and Nontarget Analysis. *Environmental Science & Technology*, **2024**, 58 (14):  
678 6402-6414.
- 679 29. Liu R, Mabury S A. Unexpectedly High Concentrations of a Newly Identified  
680 Organophosphate Ester, Tris(2,4-di-tert-butylphenyl) Phosphate, in Indoor Dust  
681 from Canada. *Environmental Science & Technology*, **2018**, 52 (17): 9677-9683.
- 682 30. Meng W, Li J, Shen J, Deng Y, Letcher R J, Su G. Functional Group-Dependent  
683 Screening of Organophosphate Esters (OPEs) and Discovery of an Abundant OPE  
684 Bis-(2-ethylhexyl)-phenyl Phosphate in Indoor Dust. *Environmental Science &  
685 Technology*, **2020**, 54 (7): 4455-4464.
- 686 31. Li J, Zhang Y, Bi R, Ye L, Su G. High-Resolution Mass Spectrometry Screening  
687 of Emerging Organophosphate Esters (OPEs) in Wild Fish: Occurrence, Species-  
688 Specific Difference, and Tissue-Specific Distribution. *Environmental Science &  
689 Technology*, **2022**, 56 (1): 302-312.
- 690 32. Xie Z, Zhang X, Xie Y, Liu F, Sun B, Liu W, Wu J, Wu Y. Bioaccumulation and  
691 Potential Endocrine Disruption Risk of Legacy and Emerging Organophosphate  
692 Esters in Cetaceans from the Northern South China Sea. *Environmental Science &  
693 Technology*, **2024**, 58 (9): 4368-4380.
- 694 33. Muir D C G, Howard P H. Are There Other Persistent Organic Pollutants? A  
695 Challenge for Environmental Chemists. *Environmental Science & Technology*,  
696 **2006**, 40 (23): 7157-7166.
- 697 34. Ye L, Li J, Gong S, Herczegh S M, Zhang Q, Letcher R J, Su G. Established and  
698 emerging organophosphate esters (OPEs) and the expansion of an environmental  
699 contamination issue: A review and future directions. *Journal of Hazardous  
700 Materials*, **2023**, 459: 132095.
- 701 35. Li L, Zhang Z, Men Y, Baskaran S, Sangion A, Wang S, Arnot J A, Wania F.  
702 Retrieval, Selection, and Evaluation of Chemical Property Data for Assessments  
703 of Chemical Emissions, Fate, Hazard, Exposure, and Risks. *ACS Environmental  
704 Au*, **2022**, 2 (5): 376-395.
- 705 36. Baskaran S, Lei Y D, Wania F. A Database of Experimentally Derived and  
706 Estimated Octanol–Air Partition Ratios (KOA). *Journal of Physical and Chemical  
707 Reference Data*, **2021**, 50 (4).
- 708 37. Bahadur N P, Shiu W-Y, Boocock D G B, Mackay D. Temperature Dependence of  
709 Octanol–Water Partition Coefficient for Selected Chlorobenzenes. *Journal of  
710 Chemical & Engineering Data*, **1997**, 42 (4): 685-688.
- 711 38. Kamel M, Williams A, *QMRF - Title: KOA model for the octanol/air partition  
712 coefficient prediction from OPERA models*. QMRF Report Q17-18-0018,  
713 ResearchGate, 2017. <http://10.13140/RG.2.2.14409.54883/1>.
- 714 39. Zhang Z, Sangion A, Wang S, Gouin T, Brown T, Arnot J A, Li L. Chemical Space  
715 Covered by Applicability Domains of Quantitative Structure–Property  
716 Relationships and Semiempirical Relationships in Chemical Assessments.  
717 *Environmental Science & Technology*, **2024**, 58 (7): 3386-3398.

- 718 40. OECD *Guidance Document on the Validation of (Quantitative) Structure-Activity*  
719 *Relationship [(Q)SAR] Models*; No. 69; Paris, 2014.
- 720 41. U.S. EPA WATERNT™ User's Guide.  
721 <https://episuite.dev/EpiWebSuite/#/help/waternt> (accessed 2024-12-10).
- 722 42. U.S. EPA MPBPVP™ User's Guide.  
723 <https://episuite.dev/EpiWebSuite/#/help/mpbpvp> (accessed 2024-12-10).
- 724 43. U.S. EPA KOWWIN™ User's Guide.  
725 <https://episuite.dev/EpiWebSuite/#/help/kowwin> (accessed 2024-12-10).
- 726 44. U.S. EPA KOAWIN™ User's Guide.  
727 <https://episuite.dev/EpiWebSuite/#/help/koawin> (accessed 2024-12-10).
- 728 45. Baskaran S, Lei Y D, Wania F. Reliable Prediction of the Octanol–Air Partition  
729 Ratio. *Environmental Toxicology and Chemistry*, **2021**, 40 (11): 3166-3180.
- 730 46. Cousins I T, Ng C A, Wang Z, Scheringer M. Why is high persistence alone a major  
731 cause of concern? *Environmental Science: Processes & Impacts*, **2019**, 21 (5):  
732 781-792.
- 733 47. Zhu Y, Tao S, Price O R, Shen H Z, Jones K C, Sweetman A J. Environmental  
734 Distributions of Benzo[a]pyrene in China: Current and Future Emission Reduction  
735 Scenarios Explored Using a Spatially Explicit Multimedia Fate Model.  
736 *Environmental Science & Technology*, **2015**, 49 (23): 13868-13877.
- 737 48. Li S, Zhu Y, Zhong G, Huang Y, Jones K C. Comprehensive Assessment of  
738 Environmental Emissions, Fate, and Risks of Veterinary Antibiotics in China: An  
739 Environmental Fate Modeling Approach. *Environmental Science & Technology*,  
740 **2024**, 58 (12): 5534-5547.
- 741 49. Zhu Y, Tao S, Price O R, Shen H, Jones K C, Sweetman A J. Environmental  
742 Distributions of Benzo[a]pyrene in China: Current and Future Emission Reduction  
743 Scenarios Explored Using a Spatially Explicit Multimedia Fate Model.  
744 *Environmental Science & Technology*, **2015**, 49 (23): 13868-13877.
- 745 50. Zhu Y, Price O R, Kilgallon J, Rendal C, Tao S, Jones K C, Sweetman A J. A  
746 Multimedia Fate Model to Support Chemical Management in China: A Case Study  
747 for Selected Trace Organics. *Environmental Science & Technology*, **2016**, 50 (13):  
748 7001-7009.
- 749 51. Zhu Y, Tao S, Sun J, Wang X, Li X, Tsang D C W, Zhu L, Shen G, Huang H, Cai  
750 C, Liu W. Multimedia modeling of the PAH concentration and distribution in the  
751 Yangtze River Delta and human health risk assessment. *Science of The Total*  
752 *Environment*, **2019**, 647: 962-972.
- 753 52. Webster E, Mackay D, Wania F. Evaluating environmental persistence.  
754 *Environmental Toxicology and Chemistry*, **1998**, 17 (11): 2148-2158.
- 755 53. Klasmeier J, Matthies M, Macleod M, Fenner K, Scheringer M, Stroebe M, Le  
756 Gall A C, McKone T, Van De Meent D, Wania F. Application of Multimedia  
757 Models for Screening Assessment of Long-Range Transport Potential and Overall  
758 Persistence. *Environmental Science & Technology*, **2006**, 40 (1): 53-60.
- 759 54. Zhu Y, Price O R, Tao S, Jones K C, Sweetman A J. A new multimedia contaminant  
760 fate model for China: How important are environmental parameters in influencing  
761 chemical persistence and long-range transport potential? *Environment*

- 762 *International*, **2014**, 69: 18-27.
- 763 55. Zhang X, Sühling R, Serodio D, Bonnell M, Sundin N, Diamond M L. Novel flame  
764 retardants: Estimating the physical–chemical properties and environmental fate of  
765 94 halogenated and organophosphate PBDE replacements. *Chemosphere*, **2016**,  
766 144: 2401-2407.
- 767 56. Wang C, Yuan T, Wood S A, Goss K U, Li J, Ying Q, Wania F. Uncertain Henry's  
768 law constants compromise equilibrium partitioning calculations of atmospheric  
769 oxidation products. *Atmos. Chem. Phys.*, **2017**, 17 (12): 7529-7540.
- 770 57. Ebert R-U, Kühne R, Schüürmann G. Henry's Law Constant—A General-Purpose  
771 Fragment Model to Predict Log Kaw from Molecular Structure. *Environmental*  
772 *Science & Technology*, **2023**, 57 (1): 160-167.
- 773 58. Nedyalkova M A, Madurga S, Tobiszewski M, Simeonov V. Calculating the  
774 Partition Coefficients of Organic Solvents in Octanol/Water and Octanol/Air.  
775 *Journal of Chemical Information and Modeling*, **2019**, 59 (5): 2257-2263.
- 776 59. Niederer C, Goss K-U. Effect of ortho-chlorine substitution on the partition  
777 behavior of chlorophenols. *Chemosphere*, **2008**, 71 (4): 697-702.
- 778 60. Wittekindt C, Goss K-U. Screening the partition behavior of a large number of  
779 chemicals with a quantum-chemical software. *Chemosphere*, **2009**, 76 (4): 460-  
780 464.
- 781 61. A. Fleckenstein C, Optimization Strategies Based on the Structure of the Analytes.  
782 In *Optimization in HPLC*, 2021; pp 141-164.
- 783 62. Matthies M, Beulke S. Considerations of temperature in the context of the  
784 persistence classification in the EU. *Environmental Sciences Europe*, **2017**, 29 (1):  
785 15.
- 786 63. Mahdi W A, Obaidullah A J. Combination of machine learning and COSMO-RS  
787 thermodynamic model in predicting solubility parameters of cofomers in  
788 production of cocrystals for enhanced drug solubility. *Chemometrics and*  
789 *Intelligent Laboratory Systems*, **2024**, 253: 105219.
- 790 64. Salthammer T, Grimme S, Stahn M, Hohm U, Palm W-U. Quantum Chemical  
791 Calculation and Evaluation of Partition Coefficients for Classical and Emerging  
792 Environmentally Relevant Organic Compounds. *Environmental Science &*  
793 *Technology*, **2022**, 56 (1): 379-391.